

TRANSIENT CONVECTIVE BOILING: ANALYSIS OF EXPERIMENTAL RESULTS

N. Baudin^{1,2}, C. Colin², P. Ruyer¹ and J. Sebilleau²

1: Institut de Radioprotection et de Sûreté Nucléaire (IRSN), PSN-RES, SEMIA, LIMAR, Cadarache, St Paul-Lez-Durance, 13115, France

2: Institut de Mécanique des Fluides de Toulouse, Allée Camille Soula, University of Toulouse Toulouse, 31400, France
nicolas.baudin@irsn.fr

ABSTRACT

During reactivity initiated accidents (RIA) in a PWR core, a power excursion occurs on some fuel rods. The consequent possible film boiling over rod's clad is a matter of study by the Institut de Radioprotection et de Sûreté Nucléaire (IRSN) for the nuclear power plants safety evaluation, because of the risk for rod's clad failure. To study the influence of power excursions on the boiling heat transfer, an experimental set-up has been built at the Institut de Mécanique des Fluides de Toulouse (IMFT). Subcooled HFE-7000 flows vertically upward in a semi annulus test section. The inner half cylinder simulates the clad and is made of a stainless steel foil, heated by Joule effect. Its temperature is measured by an infrared camera filming the backside of the foil, coupled with a high speed camera for the visualization of the flow topology.

During a typical test different heat transfer regimes are observed: forced convection, nucleate boiling and film boiling. These regimes are successively analyzed in steady and transient conditions for a large set of conditions. According to the heat transfer regime, several methods are used: flow visualization (either PIV or high speed camera pictures for bubbly flow), development of analytical model, comparison against single-phase CFD simulations, two-phase boundary layer model or correlations from the literature. Transient heat transfer are enhanced, respectively deteriorated, during stages of increasing, respectively decreasing, wall temperature, with respect to similar wall temperature steady state heat transfer.

KEYWORDS

Boiling, RIA, experimental study.

1. INTRODUCTION

Transient boiling regimes are present in various situations: cooling down of hot surfaces, chill down of pipes by cryogenic propellant before space engines re-ignition, and also in accidental situations in the nuclear power plants. In this last context the reactivity initiated accident (RIA) is one of the design basis accident considered in the safety evaluation of the light water reactors. At the fuel rod scale, it corresponds to a very fast power increase that induces soaring fuel and clad temperatures in a small part of the reactor core. The risk of clad failure during the accident has to be assessed. It is partially determined by the clad temperature transient. If boiling occurs, a vapour film can spread over the clad resulting in a deterioration of the heat transfer. Among the several past research programs on RIA performed on research reactors, the experiments conducted on the Nuclear Safety Research Reactor (NSRR) have brought some interesting insights for the determination of a transient boiling model. They show a large impact of the heating rate on the wall to fluid heat transfer, compared to steady state case.

Conditions of room temperature and ambient pressure have been analyzed in [1] but those thermal hydraulics conditions are far from those of an RIA in a pressurized water reactor. Analysis of RIA transients obtained on the NSRR facility, including high pressure cases, is still going on, including modeling attempts e.g. [2]. The tests performed on the PATRICIA facility [3], reproduced RIA clad heating rates on a simulated rod in those thermal hydraulics conditions. Their enlightening analysis has led to improved transient boiling curve model. Nevertheless, these analyses are still limited: (i) uncertainties on measurements are related to the difficulty to insert thermocouples in the wall in such conditions but, (ii), the main limitation lies in the lack of understanding of the dependency of transfer with respect to the heating rate. It is believed that, in addition to the analyses of large scale experiments like those performed on the NSRR or PATRICIA facilities, a deeper and more fundamental investigation of the process of boiling in transient conditions in a less complex environment would be beneficial.

Most of the heat transfer models for boiling flows are established for steady state conditions. Let us specify that we consider transient heat transfer conditions as those where time scale of power transient is small with respect to time scale for steady state regime establishment. The latter is not always clearly defined for a given heat transfer regime. As an illustrative example, if one considers nucleate boiling, transient conditions are achieved when the time scale for the heating of the wall is less than the typical period of a bubble nucleation growth and departure cycle in an established nucleate boiling regime. Among the few studies related to the transient boiling phenomena, some are related to explosive boiling [4], for which the time scale for heat transfer is less than the pressure relief. Those conditions do not match RIA related conditions for wall to fluid heat transfer for which the classical order of magnitude of temperature increase time is a few hundredths of second. No pressure transient is foreseen for our conditions of interest. Sakurai et al., [5] studied the boiling over a thin wire for a large spectrum of time scales and proposed different mechanisms of transition to film boiling according to the heating rate. Auracher and Marquardt, [6], performed boiling experiments over a thin horizontal disk whose transient temperature is mastered and showed that transient boiling heat flux increases with the wall temperature increase rate. The understanding is still missing and the conditions are far from those of RIA (no convection). In view of the absence of separate effect experiments that investigate high heating rates, with a representative geometry and accurate measurement devices, and of the lack of knowledge on rapid transient boiling the French "Institut de Radioprotection et de Sûreté Nucléaire" (IRSN) defined a research program. Therefore an experimental set-up has been built at the Institut de Mécanique des Fluides de Toulouse. The main objective is to study the transient boiling phenomenon over a wall simulating a fuel rod while mastering its heating rate, the bulk flow subcooling and velocity and characterizing precisely the heat transfer and the boiling incipience.

The paper is organized as follows. First, in section 2, we briefly consider the main understanding of the wall to fluid heat transfer in the flow boiling RIA context. Then we present the main features of the experimental device (section 3) and of a typical transient power test (section 4). Then heat transfer regimes are successively analyzed, both in steady (when available) and transient conditions, namely: single phase convection and onset of nucleate boiling in section 5, nucleate boiling in section 6, film boiling till rewetting in section 7.

2. SHORT STATE OF THE ART

Several in-pile experimental tests that simulate reactivity insertion accidents on nuclear fuel rods have led to high clad temperature: there has been a dry-out of the clad. The time recorded temperature measurements have clearly shown a succession of heat transfer regimes. Efficient heat exchange due to the onset of nucleate boiling is followed by a drastic decrease of the heat transfer and a very sharp temperature increase. The maximal heat transfer, a peak in the wall to fluid heat flux before the sharp temperature increase, can be very high and larger than the critical heat flux of departure from nucleate boiling type, which is the maximal heat flux of steady nucleate boiling. The temperature still increases

rapidly up to a peak that is followed by a rather smooth decrease of temperature. In the last part, a second maximum in the heat transfer occurs corresponding to a very rapid decrease of wall temperature associated to the final quench of the wall. Those experiments are still analyzed in terms of the influence of the main parameters of the test (namely pressure, enthalpy increase of the fuel, subcooling of the fluid, flowrate) on the clad peak temperature or on the duration of the dry-out of the clad (time elapsed between the two heat flux peaks). As an illustrative example, Georgenthum et al. [7] reported a clear dominant impact of the fuel enthalpy increase on the first maximal heat flux whereas flowrate or subcooling have a rather low influence on it. The maximal values reported in NSRR are always larger than the corresponding steady state critical heat flux. It is well known that flowrate and subcooling are some of the main parameters used to correlate the critical heat flux in steady conditions, e.g. [8]. In transient conditions, Sakurai et al. [9] reported that for pool conditions, in addition to the subcooling, the heating rate has a large influence on the maximal heat flux. This influence is non-monotonic and it could even lead to maximal heat flux for very high heating rates to be smaller than the corresponding steady state critical heat flux. The transient variations of the maximal heat flux before dry-out in NSRR conditions remains to be clarified.

The heat transfer coefficient in the film boiling regime during an NSRR test has been deduced from inverse heat conduction problem, [2]. Due to the subcooling and flowrates, this corresponds to the so-called Inverted Annular Film Boiling (IAFB) regime where a thin vapor film isolates the wall from the bulk liquid flow. A large standard deviation is observed for this coefficient, especially for the lowest temperature. This can be explained by transient effects: in IAFB, the thickness of the vapor film plays a major role on heat transfer. For rapid transient the time scale for its establishment or collapse could be non-negligible. Several models have been developed to describe the film boiling regime from steady state correlations, see [1,2]. In each case, an empirical factor is required to catch the correct order of magnitude of the transient heat transfer. And this heat transfer coefficient has a main impact on the peak clad temperature or on the film boiling duration as shown by Bessiron [3]. This statement is the main motivation for the present study. The understanding of the impact of the power transient on the heat transfer regime along the whole boiling curve is still under progress and we illustrate the main achievements in the following sections.

3. EXPERIMENTAL FACILITY

In this section, we introduce the main features of the facility. The experimental set-up consists of a metal half-cylinder heated by Joule effect, placed in a semi-annular section as shown in figure 1. The inner half cylinder is made of a 50 microns thick stainless steel foil that is rigid thanks to its curvature. Its diameter is 8.4mm and its length 200mm. The outer part consists of a 34mm internal diameter glass half cylinder. More details can be found in Visentini et al. [10]. The semi-annular section is filled with a coolant 1-methoxyheptafluoropropane (C₃F₇OCH₃), which will be referred as HFE7000 (3M). This fluid has been chosen because of its low saturation temperature (35°C at atmospheric pressure), its latent heat of vaporization (ten times smaller than the water one), and the reduction in the critical heat flux that it induces (for atmospheric pressure, the critical heat flux given by Zuber's correlation is 1.11MW/m² for water and 0.17 MW/m² for HFE7000). It allows reducing the required power to reach transient boiling.

There are very low heat transfers between the air and the back of the foil so this surface is assumed adiabatic. The thermal gradient across the foil thickness is expected to be negligible, since the Biot number Bi characterizing the thermal resistance of the foil by comparison to the thermal resistance of the flow is very small. For a high heat transfer coefficient $h=6000$ W/m²/K, the Biot number is equal to $Bi=h.e_w/\lambda_w=0.018$, e_w being the foil thickness and λ_w its thermal conductivity. Due to the small value of Bi , in the following the wall temperature measured by the infra-red camera at the backside of the metal foil will be considered equal to the temperature of the wall in contact with the fluid. Moreover, the diffusion time across the foil thickness, 0.6 ms, is actually small enough to assume that there is no time

lag between the thermal evolution of the outer and inner wall. Thus, it is possible to measure the temperature of the wall that is in contact with the air, in order to know the temperature of the wall that is wetted. The metal half-cylinder is glued to two lateral quartz glass plates (3 mm thickness, 42 mm width, 200 mm length). The plates, together with the foil, are placed in an aluminium cell. In this cell, a visualization box is created in order to reduce optical distortions. This box is also filled with HFE7000.

The Particle Image Velocimetry measurements are carried out in the vertical symmetry plan of the test section. The laser used is a "Nd:YAG" QUANTEL TWIN ULTRA with a wavelength of 532nm and an energy of 30mJ for two pulses of 7ns at 15Hz. Images are recorded by Sencicam PCO camera with an optical MACRO NIKON that is positioned similarly to the high speed camera on Fig. 1. The size of the CCD is 1376 x 1040 px². The mean velocities and RMS values are calculated with the software Davis. The electrical power is provided by a power supply SORENSEN SGA. It covers the 0-40V voltage range and the 0-250A current range. The power supply is driven by an arbitrary generator where all kind of curves can be programmed. The power supply can provide a current increase up to 45A/s. Voltmeter and ammeter measure the tension U and current I to calculate the generated power in the metal foil $P=UI$.

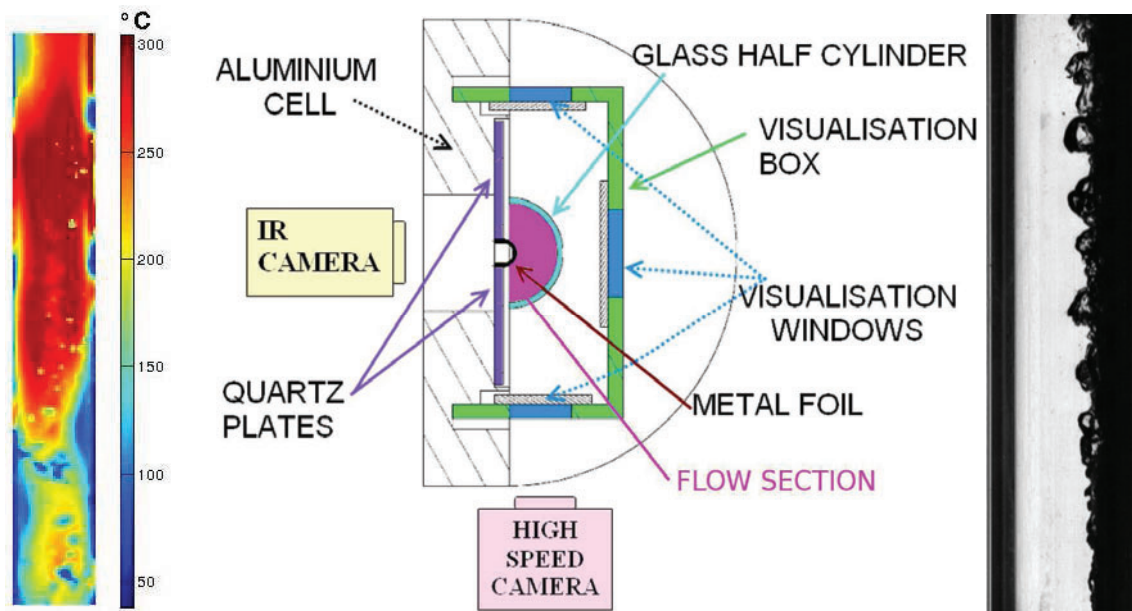


Figure 1. Cross section of the test section, IR (LHS) and high speed (RHS) camera pictures

The metal foil is painted in black in order to increase its emissivity (the emissivity of the paint is 0.94). The thermal measurements are realized by means of an infra-red camera that looks at the foil from backward (see fig. 1). The CEDIP JADE III camera with a sensitivity range is 3.5-5.1 μm is used. It has a focal plane array type and it has a Stirling-cooled MCT detector of 240x320 pixels². An acquisition frequency of 1000 im/s can be reached on small window of 64x120 pixels² while, without windowing, its highest frequency is 350 im/s. The 1000 im/s acquisition rate guarantees that the thermal dynamics is correctly followed, as the fastest heating tests have a 0.1s power rising time, and the diffusion time in the foil thickness is only 0.6 ms. The infra-red camera is calibrated thanks to a DCN 1000 N4 black body. It is possible to regulate a temperature level on this body and to film it by the camera. For the experimental tests presented, a 150 im/s frequency was chosen with a 240x320 pixels². The height of the metal foil area that was investigated was 71 mm.

The thermal measurements are coupled with high speed camera visualizations. The high-speed camera, a PHOTRON RS 3000, is directed toward one side of the half cylinder. The used acquisition rate of the

experiments was 500 im/s, with an image size of 1024x1024 pixels². The output signal of the high-speed camera is recorded by means of a National Instruments data acquisition system. By the same box, the tension and current signals are picked up and this permits to synchronize the camera images to the recording of the other measurement signals. The heat flux transmitted to the liquid is calculated from the power generated in the metal foil by Joule effect q_{gen} and from the energy stored in the foil itself. A calculation of the 2D transient heat conduction in the metal foil and the quartz plates has been performed using COMSOL Multiphysics and showed that there are limited losses toward the quartz plates. It is possible to estimate the heat flux Φ_w transferred to the fluid by a simple thermal balance:

$$\phi_w = \phi_{gen} - \rho_w C_{pw} \frac{dT_w}{dt} e_w \quad (1)$$

where $\rho_w=7930 \text{ kg/m}^3$, $C_{pw}=500 \text{ J/(kg K)}$ and e_w are the density, heat capacity and thickness of the foil, respectively. Φ_{gen} is the surface density of flux of the power supply. The National Instruments box is also used to acquire the thermocouples signals. Three K-type thermocouples measure the HFE7000, air, and infrared camera temperatures. The experiments are carried out in flow boiling conditions by inserting the test cell in a two-phase flow loop consisting of a gear pump, a Coriolis flow meter, a preheater, a 1m long channel upstream the test section to establish the flow and a condenser.

4. SKETCH OF A TEST WITH TRANSIENT POWER

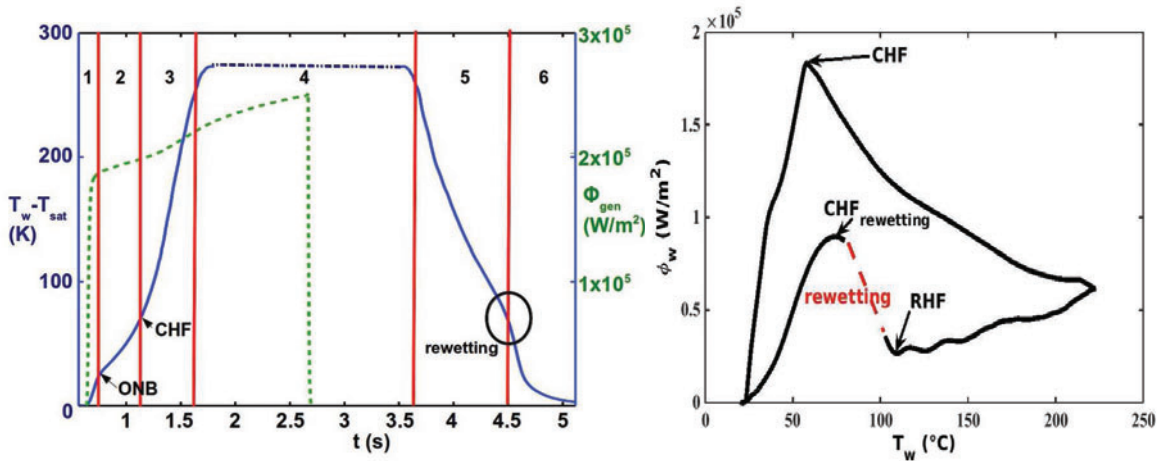


Figure 2. LHS: power (green dashed curve),and wall temperature (blue continuous curve) transients. RHS: corresponding boiling curve (power versus temperature).

Thanks to the power supply we perform a large variety of time dependant power transients, either made of successive steps or ramps. Heat transfer does depend on those power transients time variations. Among them, let us introduce a test that allows to go through the whole set of heat transfer regimes observed as well during some RIA tests as during our lab experiments. This test is performed with a power supply starting from 0 and reaching a high intensity within a short time. Actually, the power supply is not perfectly constant after the step of power and the intensity increases a little. Figure 2 - LHS shows the mean wall temperature and power curves of such a test. The Joule power is divided by the wall thickness (right ordinate scale axis of LHS figure 2). Figure 2 –RHS shows the corresponding heat flux versus the wall temperature. We can see 6 parts: the first one corresponds to the increase of the temperature in a transient convection regime. Then, nucleate boiling begins (ONB) and enhances the heat transfer, which results in a reduced temperature rise. After passing the critical heat flux (CHF), film boiling occurs, which reduces the heat transfer and induces a large increase of temperature. The temperature during part 4 does

not correspond to a physical value since the signal of the infra-red camera reaches its saturation threshold. The calibration will be improved in subsequent studies. During this part the power supply is switched off and the temperature decreases. In part 5, the temperature decreases slowly in film boiling. Past the rewetting heat flux (RHF) that corresponds to the minimum heat flux for quasi steady experiments, the fluid rewets the wall and the heat transfer gets higher. The rewetting part is more visible on the boiling curve (fig. 2). The temperature goes back to the ambient through first a nucleate boiling regime and then a single-phase regime. It is worth pointing out that such a boiling curve is very similar to those obtained during RIA tests on the NSRR facility, e.g. [7]: it justifies our interest to more deeply investigate the heat transfer processes obtained on our lab facility. To better understand the dependency of heat transfer with the power transient, we also need to accurately study the corresponding steady state heat transfer regimes.

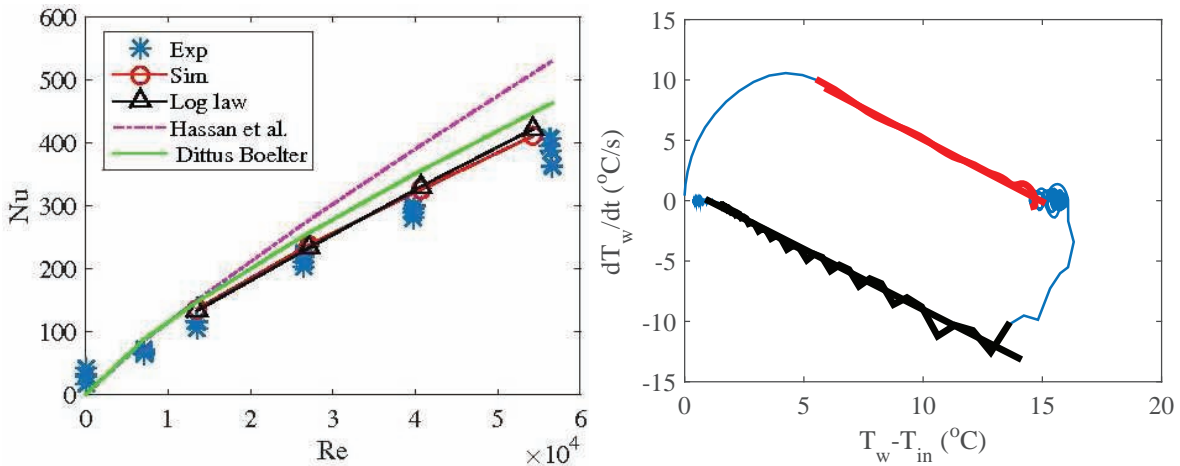


Figure 3. LHS: steady state Nusselt number as a function of the Reynolds number. Star symbols : experimental measurements, red circles: numerical simulation, black triangle : log law theoretical model, dashed line: Hassan et al. correlation, continuous line : Dittus-Boelter correlation; RHS: wall temperature transient during a rectangular function power transient : temperature variation rate as a function of the difference between inlet flow temperature and wall temperature (0°C for 0 power and around 15°C for the power level of this test).

5. FROM CONVECTION TILL BOILING

5.1. Transient convection

During the part 1 of a test, the flow in the test section is established and the power is set on. The heat transfer and flow have been studied thanks to experiments, numerical simulations, and correlations [11]. Let us present the main results. Using the PIV measurements, we studied the velocity profile across the semi-annular duct along the axis in the symmetry plane of the fluid section. It is similar to the theoretical profile in an annular duct (of same inner and outer diameter and maximum velocity) as studied by Kaneda et al. [12]. We considered the numerical simulation of the flow within the whole flow domain with a $k-\epsilon$ turbulence model and a low Reynolds law near the walls using StarCCm+. Mean and RMS velocities as measured by PIV are very well captured by the numerical simulations. It shows that this similarity in profiles is still true over a large angle portion ($\pm \pi/4$) of the semi-annular around the symmetry axis. For each azimuth, the maximal velocity is closer to the inner wall where the shear stress is larger (than at the outer wall). The friction factor value is consistent with values of the literature.

For the heat transfer with constant wall to fluid heat flux, numerical simulations have been performed till steady state. The obtained Nusselt variation with respect to the Reynolds number is very close to the one

obtained during our experiments. It is close to the one obtained on annular by Hassan et al. [13] and bounded by the classical Dittus-Boelter correlation for cylinders as illustrated by the LHS picture of Fig. 3. Its azimuthal dependency has been numerically studied and is low in the $\pm \pi/4$ angular sector around symmetry like the one previously mentioned for the velocity profile.

The transient convection has been analyzed for a rectangular function type power signal. From the experimental measurements as well as from the numerical simulations, a time scale can be clearly defined since the time evolution is quasi exponential. This is illustrated in the RHS of Fig. 3 for the experimental case where the rate of wall temperature time evolution is plotted against the difference between wall and inlet temperature. In both the experimental and the numerical cases, this time scale decreases, with a similar law, when the Reynolds number increases. So far, we failed to reach a good quantitative agreement between both estimations. Nevertheless, we have shown how this time scale is related to the growth rate of the thermal boundary layer. This allows defining a clear boundary between steady and transient cases.

5.2. Onset of nucleate boiling (ONB)

Let us consider a power step such that wall temperatures reaches values significantly above the liquid saturation temperature, heterogeneous nucleation can occur, leading to the onset of nucleate boiling. This time can be clearly identified since the wall temperature suddenly drops. The difference between the temperature at the onset of nucleate boiling T_{ONB} and the saturation temperature T_{sat} , and the time needed to observe nucleate boiling t_{ONB} (till the power has been turned on) are shown in figure 4 for several tests. We can see that $T_{ONB}-T_{sat}$ increases with Φ_{gen} whereas t_{ONB} decreases. Let us precise that in the transient convection regime, the wall temperature is not spatially homogeneous along the wall. The results discussed in this part are obtained for a distance of about $15cm$ from the bottom of the heated wall.

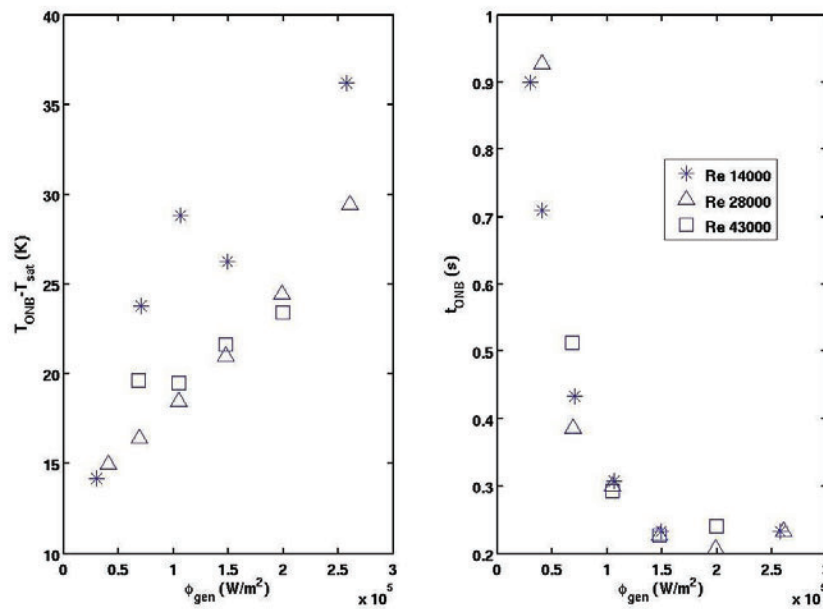


Figure 4. Temperatures and times at onset of nucleate boiling for different power levels and flowrates

In [14], we studied a model of wall temperature at the onset of nucleate boiling for transient heating. In a first attempt, we considered a transient adaptation of the Hsu model. The model of Hsu [15] predicts the

heterogeneous nucleation for a given cavity size in a thermal boundary layer. It considers that the onset of boiling occurs when the top of the bubble, which size depends on the cavity size, is at a temperature of equilibrium, say T_{eq} . From the previously described numerical simulations of the transient convection, we can evaluate the time for which the Hsu's model criterion of onset is reached as a function of the cavity size r_c . This induces a variation of the wall temperature at the onset of nucleate boiling with respect to the power transient, say Φ_{gen} . The steady state value of the classical Hsu model is also found naturally. The cavity size remains an unknown parameter in the Hsu's model. Fitting the cavity size in the Hsu model to match the correct rate of variation of T_{ONB} with Φ_{gen} leads to (i) large values for T_{ONB} and (ii) an unrealistic cavity size with respect to the typical roughness of around $1\mu\text{m}$ of the wall in our experiments. For realistic sizes of cavity, the top of the bubble is too close to the heated wall to obtain a variation of temperature between the top and the bottom of the bubble in the thermal boundary layer: no transient effect should be observed on T_{ONB} that is in contradiction with our experimental results.

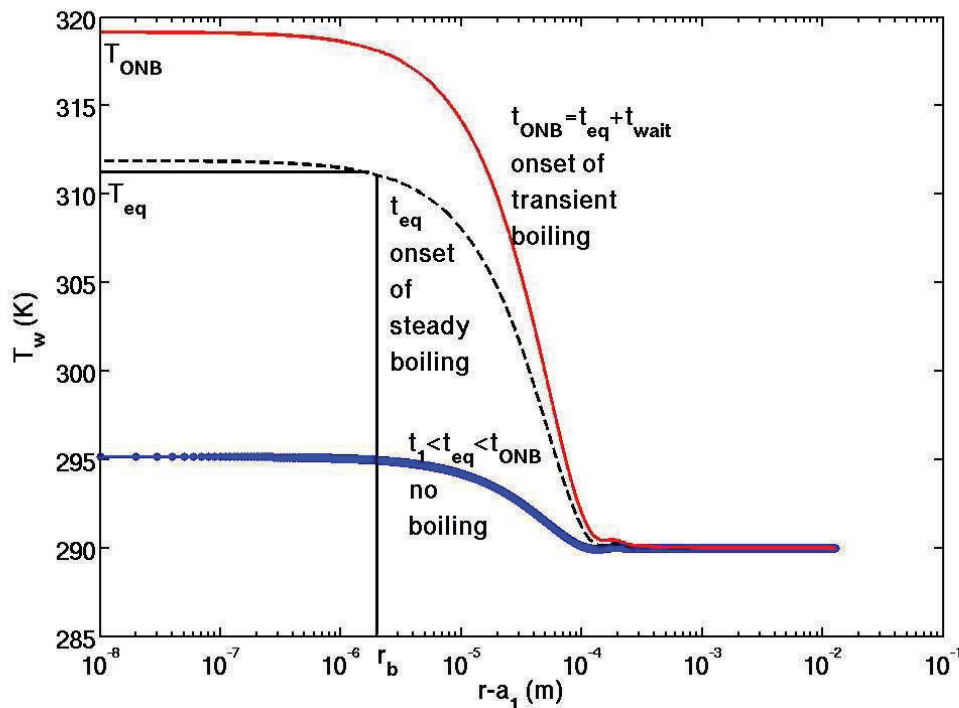


Figure 5. Evolution of the fluid temperature versus the position in the fluid: model of ONB with a waiting time ($r-a_1$ is the radial coordinates in the semi-annular duct)

In this first attempt, we considered that a given time, say t_{eq} , was needed to obtain the thermal boundary layer. This is actually a lower limit for the nucleation process since it neglects the heat and mass transfer kinetics associated to the bubble nucleation. During this additional process leading to the actual onset of nucleate boiling, the wall temperature still increases for transient cases. This statement is supported by our observation that a threshold of energy per wall surface unit (around $20000\text{J}/\text{m}^2$) has to be transferred to the fluid before nucleate boiling can occur, [10]. This led us to introduce an additional time, say t_{wait} , to roughly model this effect. Figure 5 illustrates the model with the evolution of the fluid temperature versus the radial position in the liquid: a temperature profile at a time $t_1 < t_{eq}$ corresponds to a moment when the wall temperature is inferior to T_{eq} and so there is no nucleate boiling. The equilibrium temperature is reached at the r_b distance from the wall at t_{eq} . (second profile) The last profile corresponds to the one after the additional period t_{wait} and corresponds to our model for the onset of boiling in transient heating cases. In transient conditions, the wall temperature increases during the time t_{wait} before actual onset of boiling.

T_w at the onset of boiling is thus larger in transient condition than in steady condition. This model is still valid in the steady state case: the temperature is constant during t_{wait} so the wall temperature at the onset of nucleate boiling is equal to the one provided by the Hsu's model. Figure 6 shows the comparison with the experimental data and the results of this model using the temperature profiles of our transient convection study. In our case, the mean rate of increase of the wall temperature $(T_{ONB}-T_{w0})/t_{ONB}$ varies, according to Φ_{gen} and Re from about $25K/s$ to $250K/s$. To fit the experimental data, the waiting time has to be varied according to the Reynolds number: $100ms$, $70ms$ and $60ms$ for the Reynolds numbers values 14000 , 28000 and 43000 . This variation is consistent with the initial concept: this waiting time represents an additional time to store an amount of energy sufficient for the bubbles to grow. Therefore, since when the Reynolds number increases, the convective heat transfer is more efficient, t_{wait} decreases. Analysis of the numerical results shows that this time allows creating a superheated layer from about $30 \mu m$ for the low heat flux to $60 \mu m$ for the higher heat flux. These lengths scales agree well with our case since they are between the roughness of the wall material ($\sim 1 \mu m$) and the size of the bubbles ($0.1/1 mm$). A further study of the bubble growth and detachment time as a function of the power supply and the fluid velocity is still required to base this time estimation on a more physical background.

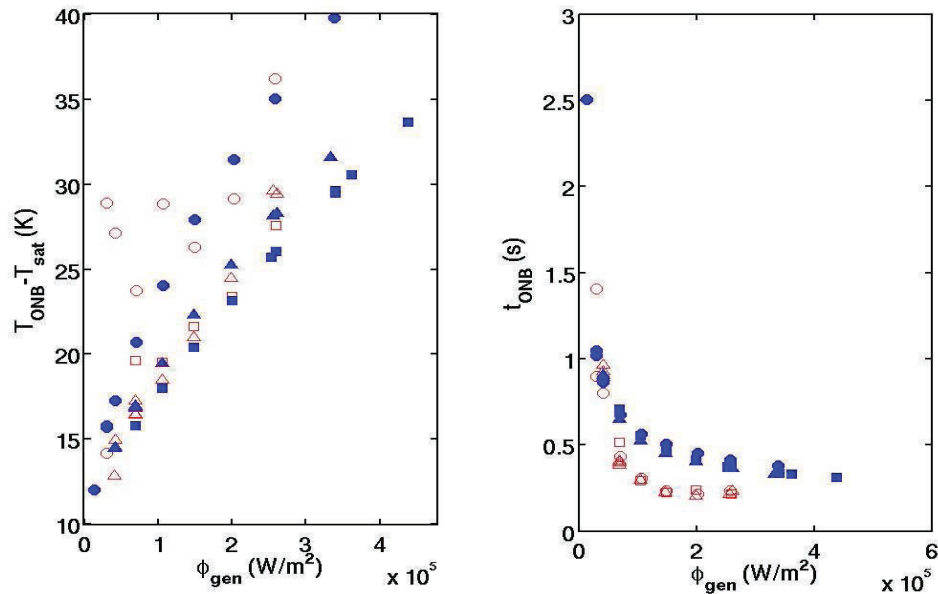


Figure 6. Temperatures and times of onset of nucleate boiling predicted by the model with a waiting time and compared with the experimental data for different power generations and fluid velocities (squares: Re=43000, triangles: Re=28000, circles: Re=14000, Experiment in red and model in blue)

6. NUCLEATE BOILING

6.1. Steady-state nucleate boiling

The pool nucleate boiling heat transfer in our test section had been correlated with success thanks to the Forster Zuber correlation, [10]. Following the Chen model for convective nucleate boiling heat transfer, we assume that it is the sum of a convective term and a nucleate boiling heat flux, namely the Foster-Zuber correlation, lowered by a suppression factor S . The Hassan et al. correlation is used since it has been successful to predict convective heat transfer (see the hereinabove section). LHS figure 7 shows the experimental data for a Reynolds number of 26,000 and a sub cooling about $5 K$, which are well predicted by the Chen's correlation. The forced convection and pool boiling contributions are also shown. In this case, the onset of nucleate boiling occurs for $T_w - T_{sat} \sim 8 K$. In the nucleate boiling regime, the wall

temperature is homogeneous with the height, thus the plotted temperature is an averaged value in the middle height of the wall. As far as steady convective nucleate boiling is concerned, we consider that we can predict the wall to fluid heat transfer in the test section thanks to classical correlations.

6.2. Transient nucleate boiling

Transient regimes are first obtained by modifying (increasing and then decreasing) the power supply steps by steps. This is illustrated by the bottom graph of the RHS of Fig. 8. These transient regimes correspond to transitions between steps of steady state regimes of nucleate boiling. The corresponding wall temperature transient is illustrated by the graph in the middle of the RHS of Fig. 8. It can be clearly seen that at the beginning of the test ($t < 10s$) the temperature does not reach a steady state value and the time scale of the temperature transient is large. These data correspond actually to convective heat transfer. At $t = 10s$, there is a sudden drop in the wall temperature that corresponds to the onset of nucleate boiling. The transient convective nucleate boiling is analyzed from this point. For transient heating and cooling corresponding to wall temperature variation rates between $-10K/s$ and $10 K/s$, the measured heat flux is compared with the heat flux calculated in a steady state with the Chen's correlation at the instantaneous wall temperature. The corresponding data plotted in RHS of figure 7 show that when the wall is heated, the transient heat flux is larger than the steady one and when it is cooled, the transient heat flux is smaller. This result was already observed in the literature (Auracher and Marquardt [6], Visentini et al. [10]). It seems that the ratio observed in the present conditions is smaller than the results of Auracher et al. and Visentini et al. It may be due to differences in the experimental conditions: Auracher et al. control the wall temperature and Visentini et al. performed experiments with high fluxes, larger than steady states boiling conditions.

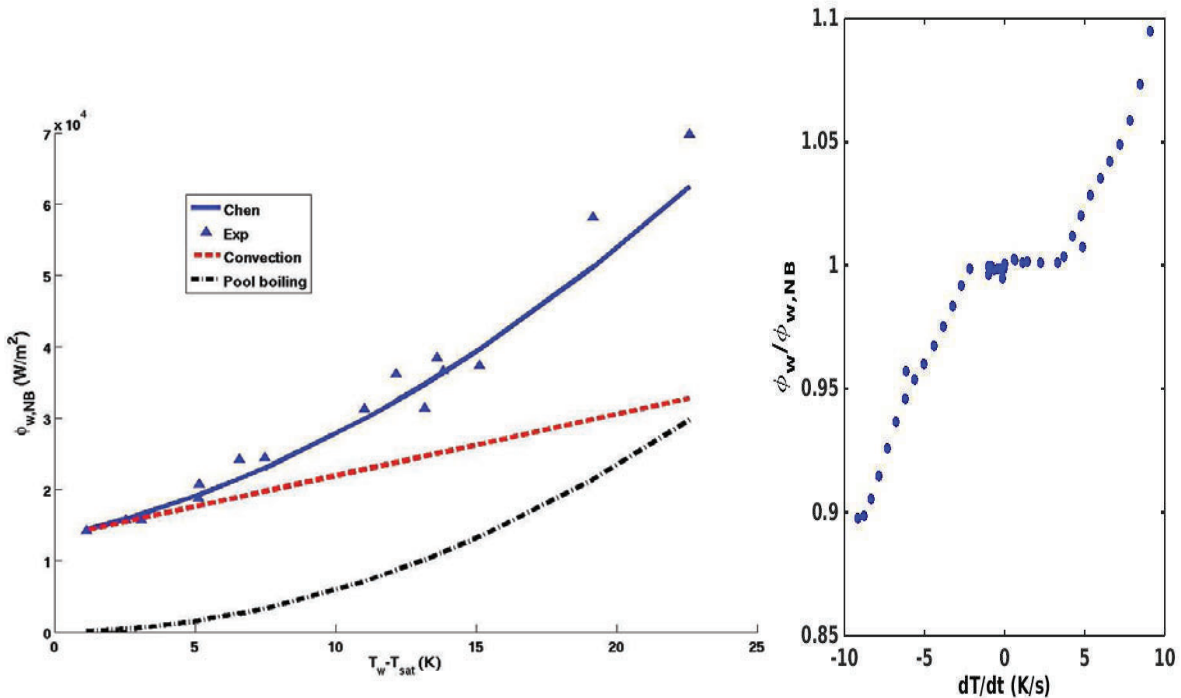


Figure 7. LHS: Boiling curve for a flow $Re=26\ 000$, $T_{sat}-T_l \sim 5K$. Forced convection and pool boiling contributions in Chen's correlation are plotted; RHS: Ratio between instantaneous measured Φ heat flux and the corresponding Φ_{NB} versus the wall temperature variation rate

An attempt to relate these measurements to visual observation of the two-phase flow topology has been made: using high speed camera visualizations, we define a bubble layer size. This bubble layer is obtained from images on Matlab software. First the background is subtracted to the image and the image is cropped to remove the wall. Then using the *bwboundaries* function and retaining the largest boundary allows obtaining the bubble layer near the wall without taking account bubbles that have already detach in the flow. LHS of Figure 8 shows such a picture analysis : original photo on the LHS and boundary of the bubble layer in red plot on the RHS. Top graph of the RHS of Figure 8 shows the mean size of the bubble layer d_b on a small area versus time. We clearly see the onset of nucleate boiling around $t=10$ s. The thickness of the bubbly layer increases over a short time following a power step and then remains stable. The time scale for the bubbly layer thickness transient is smaller than the one deduced from the wall temperature transient.

We also performed experiments with higher power steps that cannot lead to steady nucleate boiling (since the corresponding wall to fluid heat flux is too large). The figure 9 shows the mean thickness of the bubble layer, the mean wall temperature on a small area and the Joule heat flux versus time. During the time when bubbles are present, the wall temperature varies linearly with time. Because of the wall thickness and the Joule power heating, the heat flux is constant (see section 3). The bubble layer thickness stays constant too and we can guess that in a configuration with a Joule heating, the transient nucleate boiling is governed by the heat flux more than by the wall temperature. With the numerical simulations we saw that the superheated layer is about 20/50 μm when the bubble layer thickness is about 0.1/1 mm. It could be the result of a competition between the evaporation at the bottom of the bubble and condensation at the top which sets the bubble size, and so the heat flux. If this heat flux is below the Joule power, the wall temperature will increase.

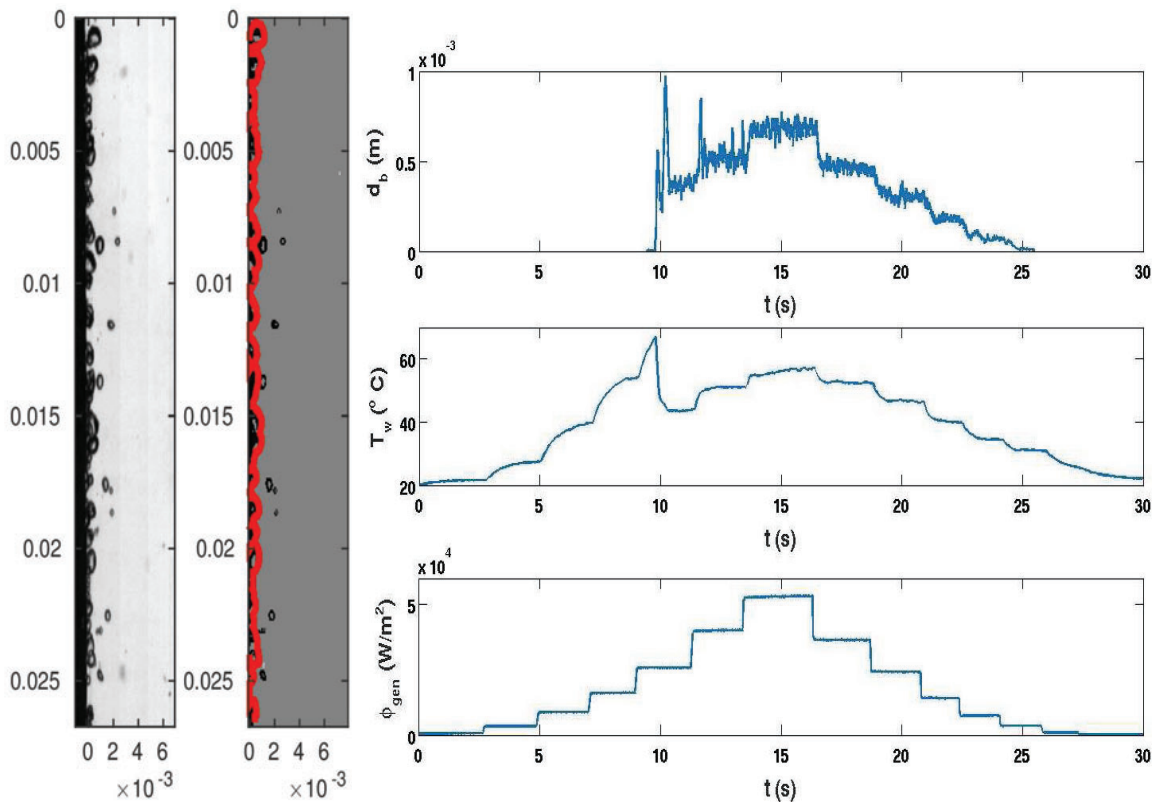


Figure 8. LHS: Raw picture of the high speed camera (left) and the calculated bubble layer (red curve); RHS: Mean bubble layer thickness, mean wall temperature and Joule heat flux versus time.

Figure 9 RHS shows the rate of the wall temperature increase as a function of the power generation during such transient nucleate boiling. We can see that the tests with a Joule power above about 50kW/m^2 are transient. Three flow rates are considered. Highest Reynolds numbers cases are equivalent while the increase rate for the lowest is higher for a same heat flux. This is consistent with our observations concerning the convection characteristic time and t_{wait} : they are smaller and very similar for the highest Reynolds numbers case with respect to the lowest.

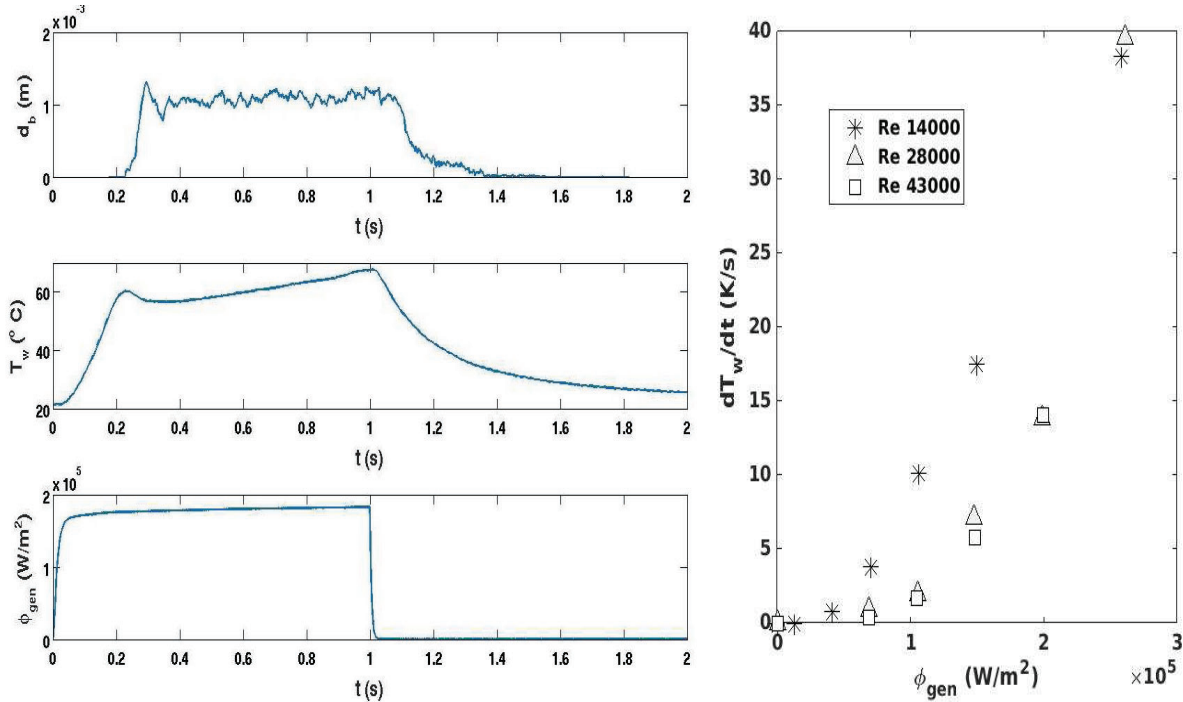


Figure 9. LHS: Mean bubble layer thickness, mean wall temperature and Joule heat flux versus time. RHS: wall temperature increase rate as a function of power level

7. FILM BOILING

The onset of the film boiling can be mainly achieved according to two different processes: either a direct transition from non-boiling to film boiling for very large heating rates, or from a nucleate boiling regime. Study of this transition is still under progress and the value of a steady-state critical heat flux is not available. In this paper, we focus on the analysis of the last part of the film boiling regime till rewetting (part 5). The vapor film collapse corresponds to a sharp transition of heat transfer regime and a large temperature drop. Since the associated quench front velocity is of the order of 10cm/s , there exist strong temperature and heat transfer differences over the wall. This implies that a local analysis is required to correctly interpret the data. On the LHS of Fig. 10, such local boiling curve during are represented at 3 different axial locations. As it can be seen on the corresponding temperature curves (RHS), it corresponds to a less than 1 second elapsed time under the film boiling regime.

A two-layers axial model for inverted annular film boiling has been solved dynamically similar to other studies [16,17]. It considers mass, momentum and energy balances across the vapor film whose thickness varies axially and in the liquid bulk flow. Initial conditions are experimentally determined in terms of axial profiles for wall temperature and vapor film thickness (that lies between $0.5 \cdot 10^{-4}\text{m}$ and 10^{-4}m). The quench front corresponds to a zero vapor film thickness, and the corresponding rewetting temperature (*i.e.*

the Leidenfrost point of our experiment) is assumed to be equal to 90°C. As it can be seen on the RHS curve of fig. 10, the model provides a very good estimation for the rate of temperature decrease till rewetting and on its axial variations. The quench front progression and the vapour film thickness evolutions are in correct agreement with experimental observations as well.

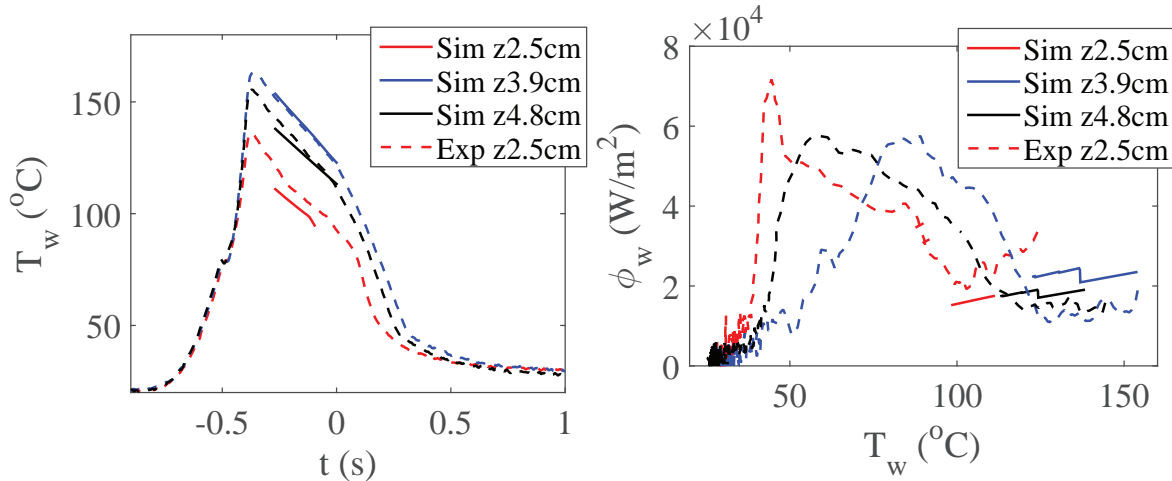


Figure 10. Local boiling curve for part 5-6 (RHS) and whole wall temperature history (LHS) at different vertical locations. Continuous lines: model; dashed lines: experimental measurements.

CONCLUSIONS

This experimental study is motivated by the lack of knowledge about the dependency of boiling heat transfer in transient conditions. This has been shown to be a dominant effect on the fuel rods temperature transient following a reactivity insertion accident. The experimental facility used in the present study allows to reproduce a power transient leading to a succession of transient boiling regimes similar than those observed during in-pile experiments.

Convective heat transfer has been finely analyzed both in steady and transient conditions. It allows validating the choice of the semi-annular geometry as a good model for an annular flow around a rod. We validated numerical simulations of the flow and heat transfer and were thus able to predict the thermal boundary layer time and space evolution. The characteristic time for convective heat transfer to establish has been determined as a function of the Re number and qualitatively related to the latter thermal boundary evolution.

Onset of nucleate boiling in transient convective conditions depends on both the power level and the flowrate. From an adaptation of the Hsu model valid for steady conditions, we developed a model to predict the wall temperature at onset. It is deduced from the experimental observation of a required threshold of energy to set boiling on and from the study of the thermal boundary layer thickness evolution with Re in transient conditions. A characteristic time for the nucleation process has to be fitted and leads to values in good agreement with the thermal process in the near wall liquid.

When transient, the convective nucleate boiling heat transfer coefficient is higher, respectively lower, than the steady state value according to the fact that the wall temperature is increasing, respectively decreasing, with time. This can be observed for a large range of instantaneous power increase levels. The wall bubbly layer thickness has been estimated. It depends on the wall to fluid heat flux. The characteristic time scale for the establishment of this thickness is smaller than the one for the wall temperature.

Established film boiling regime till rewetting has been studied locally since heat transfer has been shown to depend on the distance to the film vapor collapse. The heat transfer has been correctly evaluated thanks to a boundary layer model.

Several studies are still under progress on the obtained results and more specifically concerning the ability to obtain steady state film boiling data or to correlate the maximal heat flux and temperature peak with transient characteristics.

REFERENCES

1. V. Besson, T. Sugiyama, and T. Fuketa, "Clad to coolant heat transfer in NSRR experiments", *Journal of Nuclear Science and Technology*, **44**(5), pp. 723-732 (2007).
2. Y. Udagawa, T. Sugiyama, M. Suzuki, and M. Amaya, "Experimental analysis with RANNS code on boiling heat transfer from fuel rod surface to coolant water under Reactivity Initiated Accident conditions", *Proc. IAEA Technical Meeting*, Chengdu, China, Oct. 2013 (2013).
3. V. Besson, "Modelling of Clad-to-Coolant Heat Transfer for RIA Applications", *Journal of Nuclear Science and Technology*, **44**(2), pp. 211-221 (2007).
4. S. Glod, D. Poulikakos, Z. Zhao, and G. Yadigaroglu, "An investigation of microscale explosive vaporization of water on an ultrathin Pt wire", *Int. J. of Heat Mass Transf.*, **45**(2), pp. 367-379 (2002).
5. A. Sakurai, M. Shiotsu, K. Hata, and K. Fukuda, "Photographic study on transitions from non-boiling and nucleate boiling regime to film boiling due to increasing heat inputs in liquid nitrogen and water", *Nucl. Eng. Design*, **200**(1-2), pp. 39-54 (2000).
6. H. Auracher, and W. Marquardt, "Experimental studies of boiling mechanisms in all boiling regimes under steady-state and transient conditions", *Int. J. of Thermal Sciences*, **41**(7), pp. 586-598 (2002).
7. V. Georgenthum, N. Trégourès, and Y. Udagawa, "Synthesis and Interpretation of Fuel Cladding Temperature Evolution under Reactivity Initiated Accident in NSRR Reactor", *Proceedings of WRFPM 2014*, Sendai, Japan, Sep. 14-17, 2014, Paper No. 100097 (2014)
8. D.C. Groeneveld, L.K.H. Leung, P.L. Kirillov, V.P. Bobkov, I.P. Smogalov, V.N. Vinogradov, X.C. Huang, and E. Royer, "The 1995 look-up table for critical heat flux in tubes", *Nucl. Eng. Des.*, **163**, pp. 1-23 (1996).
9. A. Sakurai, "Mechanisms of transitions to film boiling at CHF's in subcooled and pressurized liquids due to steady and increasing heat inputs", *Nucl. Eng. Design*, **197**(3), pp. 301-356, (2000).
10. R. Visentini, C. Colin, and P. Ruyer, "Experimental investigation of heat transfer in transient boiling", *Experimental Thermal and Fluid Science*, **Vol. 55**, pp. 95-105 (2014).
11. N. Baudin, C. Colin, P. Ruyer, and J. Sebilliau, "Turbulent flow and transient convection in a semi-annular duct", *Submitted to the Int. J. of Heat Mass Transf.* (2015).
12. M. Kaneda, B. Yu, H. Ozoe, and S.W. Churchill, "The characteristics of turbulent flow and convection in concentric circular annuli. Part I: flow", *Int. J. of Heat and Mass Trans.*, **46**(26), pp. 5045 – 5057 (2003)
13. A. Hassan, R. Roy, and S. Kalra, "Heat transfer measurements in turbulent liquid flow through a vertical annular channel", *ASME Journal of Heat Transfer*, **112**, pp. 247 – 250 (1990).
14. N. Baudin, C. Colin, P. Ruyer, and J. Sebilliau, "Experimental study of transient nucleate boiling", *9th Int. Conference on Boiling and Condensation Heat Transfer*, Boulder, Colorado, April 26-30 (2015)
15. Y. Hsu, "On the size range of active nucleation cavities on a heating surface", *ASME Journal of Heat Transfer*, **84**, pp. 207-216 (1962).
16. V. P. Carey, *Liquid-vapor phase-change phenomena*, chap. 7 Pool boiling, Taylor and Francis (1992)
17. M. Shiotsu, and K. Hama, "Film boiling heat transfer from a vertical cylinder in forced flow of liquids under saturated and subcooled conditions at pressures", *Nucl. Eng. Design*, **200**, pp. 23-38 (2000).